

East Tennessee State University

Digital Commons @ East Tennessee State University

Undergraduate Honors Theses

Student Works

5-2022

Neuroanatomical Distribution of Neurons within the Hypothalamic Paraventricular Nucleus that Project to the Brainstem Rostral Ventrolateral Medulla

Nicolas Fuller

Follow this and additional works at: <https://dc.etsu.edu/honors>



Part of the [Cardiovascular System Commons](#), and the [Nervous System Commons](#)

Recommended Citation

Fuller, Nicolas, "Neuroanatomical Distribution of Neurons within the Hypothalamic Paraventricular Nucleus that Project to the Brainstem Rostral Ventrolateral Medulla" (2022). *Undergraduate Honors Theses*. Paper 681. <https://dc.etsu.edu/honors/681>

This Honors Thesis - Open Access is brought to you for free and open access by the Student Works at Digital Commons @ East Tennessee State University. It has been accepted for inclusion in Undergraduate Honors Theses by an authorized administrator of Digital Commons @ East Tennessee State University. For more information, please contact digilib@etsu.edu.

EAST TENNESSEE STATE UNIVERSITY DEPARTMENT OF HEALTH SCIENCES

Neuroanatomical Distribution of Neurons within the Hypothalamic Paraventricular
Nucleus that Project to the Brainstem Rostral Ventrolateral Medulla

By

Nicolas F. Fuller

An Undergraduate Thesis Submitted in Partial Fulfillment
of the Requirements for the
University Honors in Discipline Program
Honors College
and the
Honors-in Health Sciences, Human Health
College of Public Health
East Tennessee State University

Nicolas Fuller

Nicolas Fuller (Apr 29, 2022 01:05 EDT)

04/29/2022

Nicolas F. Fuller

Date

Matthew Zahner

04/29/2022

Dr. Matthew R. Zahner, Thesis Mentor

Date

Eric Beaumont

04/29/2022

Dr. Eric Beaumont, Reader

Date

Michelle Chandley

04/29/2022

Dr. Michelle Chandley, Reader

Date

EAST TENNESSEE STATE UNIVERSITY DEPARTMENT OF HEALTH SCIENCES

NEUROANATOMICAL DISTRIBUTION OF NEURONS WITHIN THE
HYPOTHALAMIC PARAVENTRICULAR NUCLEUS THAT PROJECT TO THE
BRAINSTEM ROSTRAL VENTROLATERAL MEDULLA

By

NICOLAS F. FULLER

A Thesis Submitted to the
Department of Health Sciences and Honors College

Degree Awarded:
Spring 2022

TABLE OF CONTENTS

List of Figures.....	4
Abstract.....	5
1. Introduction.....	6
2. Review of Literature	7
3. Methods.....	18
4. Results.....	22
5. Discussion.....	26
APPENDIX A.....	29
REFERENCES	36

LIST OF FIGURES

1. Brainstem Microinjections.....	29
2. Nissl Stain Images of PVN.....	30
3. Ventral Parvocellular (PaV) Subnucleus	31
4. Dorsal Cap Parvocellular (PaDC) Subnucleus	32
5. Medial Parvocellular (PaMP) Subnucleus.....	33
6. Posterior Parvocellular (PaPO) Subnucleus.....	34
7. Summary Retrograde Labeling... ..	35

ABSTRACT

The sympathetic nervous system is important in maintaining cardiovascular homeostasis. Elevated cardiovascular-related sympathetic activity can lead to neurogenic hypertension and a host of other serious cardiac-related abnormalities. The paraventricular nucleus (PVN) of the hypothalamus plays an important role in sympathetic cardiovascular regulation. Neurons from the PVN project to the rostral ventrolateral medulla (RVLM), which is the main brain stem sympathetic cardiovascular control center. While RVLM-projecting PVN neurons have been well characterized, the topographical organization within the PVN subnuclei is still not fully known. This neuroanatomical study aimed to map the topographical distribution of RVLM-projecting PVN neurons. Four different carboxylate FluoSphere™ retrograde tracers (blue, 365/415; green, 505/515; red, 565/580; and far-red, 660/680) were injected at different rostro-caudal coordinates within the RVLM. The vast majority of RVLM-projecting PVN neurons were ipsilateral and located in the medial parvocellular subnucleus. Whereas most neurons were ipsilateral, there is a small fraction of neurons that crossed the midline. RVLM-projecting neurons were also identified within the dorsal, ventral, and posterior parvocellular subnuclei of the PVN with no labeling found in the anterior parvocellular or magnocellular subnuclei. Additionally, we observed different efficiencies of the retrograde tracers with blue (365/415) being the least efficient and red (565/580) being the best. These neuroanatomical data will serve as important preliminary data for future research investigating the functional and histochemical properties of these PVN neurons.

CHAPTER ONE

INTRODUCTION

Hypertension is a primary contributor to heart failure which is the leading cause of death worldwide [1,2]. Activation of the sympathetic nervous system increases heart rate and blood pressure. When the sympathetic nervous system becomes chronically overactive it can lead to neurogenic hypertension [1,2]. A better understanding of the neural pathways involved is important to the etiology and treatment of neurogenic hypertension.

The hypothalamic paraventricular nucleus (PVN) has been shown to be an important autonomic site mediating the sympathetic functions in cardiovascular regulation. Previous studies have shown that activation of the PVN results in increased blood pressure and rate of respiration [12]. The rostral ventrolateral medulla (RVLM) is the primary sympathetic cardiovascular control center that regulates blood pressure. Excitation of the RVLM increases heart rate and blood pressure [21,22]. Previous studies have shown that the PVN projects to the RVLM [12,17,18]. The aim of our study was to identify which subnuclei of the PVN contain these RVLM-projecting neurons. To do this, we bilaterally microinjected four different retrograde tracers (FluoSpheres™) into the RVLM. We identified which PVN subnuclei contained labeled RVLM-projecting neurons using fluorescent microscopy.

CHAPTER TWO

REVIEW OF LITERATURE

Autonomic Regulation of the Cardiovascular System

The parasympathetic and sympathetic nervous systems both act to maintain cardiovascular homeostasis. The parasympathetic nervous system is most active when there are no stress-inducing stimuli detected and the body is in a relaxed state. The sympathetic nervous system is activated in the event of a perceived emergency to prepare the body for energy expenditure [1]. The activity of the sympathetic nervous system is also vital in maintaining cardiovascular function on a moment-to-moment basis [2]. The degree to which the parasympathetic or sympathetic nervous system gets activated is dependent upon the type of stimuli encountered in both the external and internal environments [1].

Sympathetic activation increases cardiac output, systemic blood pressure, and the rate of respiration. Sympathoexcitation of the sinoatrial node, myocardium, and atrioventricular node causes an increase in heart rate, stroke volume, and atrioventricular conduction velocity which all contribute to the elevated cardiac output [1,4]. Sympathetic activation of the blood vessels causes vasoconstriction which increases blood pressure [5]. Activation of the sympathetic nervous system also causes bronchodilation which facilitates the increased rate of respiration [6,7].

Sympathetic Mechanisms of Cardiovascular Regulation

Cardiovascular sympathetic regulatory mechanisms rely on the relationship between receptors, control centers in the central nervous system, and effector organs. There are two primary sources of afferent input relevant to sympathetic cardiovascular regulation: chemoreceptors and baroreceptors [8]. Chemoreceptors are sensory receptors that detect changes in oxygen, carbon dioxide, and pH levels in the body. Peripheral chemoreceptors are sensory receptors of the peripheral nervous system found in the aortic bodies and carotid bodies. Central chemoreceptors are sensory neurons of the central nervous system found in various regions in the brain and brainstem, primarily on the surface of the ventrolateral medulla. Arterial baroreceptors in the aortic arch and carotid sinuses are mechanoreceptor sensory neurons that detect a change in arterial blood pressure [1].

The cardiorespiratory chemoreflex occurs in response to hypoxemia (low oxygen levels in the blood) and hypercapnia (excess levels of carbon dioxide in the blood). When activated by a change in the level of oxygen, carbon dioxide, or pH, peripheral chemoreceptors in the carotid and aortic bodies send action potentials through their afferent fibers in cranial nerves IX and X respectively [1]. These afferent fibers relay their sensory information to secondary interneurons in the nucleus tractus solitarius (NTS) in the dorsal medulla which manages various visceral afferent sensory inputs. The NTS then relays this information to respiratory control centers and both directly and indirectly to the rostral ventrolateral medulla (RVLM). From here, efferent signals from the RVLM travel to the intermediolateral column (IML) of the spinal cord to synapse with the sympathetic preganglionic motor neurons [9]. The NTS also sends axonal projections to the

paraventricular nucleus in the hypothalamus (PVN). The PVN sends projections directly to the IML as well as the RVLM and can therefore affect sympathetic activity directly through the spinal cord or indirectly through its projections to the RVLM. The PVN also sends projections to the pre-Botzinger complex and phrenic motor neurons which are both important in controlling ventilation [12]. Central chemoreceptors are primarily activated in response to increased levels of carbon dioxide (hypercapnia) and decreased pH in the interstitial fluid and cerebrospinal fluid in the brain. These receptors send their sensory information to the respiratory control centers in the brainstem and to the sympathetic regions, primarily the RVLM [10].

The arterial baroreflex is the primary mechanism of control by which the autonomic nervous system regulates short-term blood pressure. Primary afferent fibers of the arterial baroreceptors in the carotid sinuses and aortic arch continuously send impulses through the glossopharyngeal nerve (CN IX) and the vagus nerve (CN X) respectively [9]. These impulses are received by secondary interneurons in the NTS and then relayed directly to the nucleus ambiguus (NA) in the medulla, which contains parasympathetic cardiac vagal motor neurons. Here, in the event of high blood pressure, the parasympathetic nerve activity is increased to lower heart rate. The NTS also projects the impulses to interneurons in the caudal ventrolateral medulla (CVLM) which sends inhibitory projections to the sympathetic premotor neurons in the RVLM [9]. Increased baroreceptor activity inhibits the sympathetic outflow to the heart and vasculature which lowers blood pressure. When baroreceptor activity is attenuated, however, parasympathetic vagal activity is decreased while sympathetic activity in the RVLM is increased to raise arterial blood pressure [9].

Sympathetic activation in response to conditions such as hypoxemia, hypercapnia, and hypotension relies primarily on the same basic mechanisms of action. Sympathetic activation increases ventilation, cardiac output, and blood pressure [10]. Sympathetic stimulation is coupled with augmented phrenic nerve activity resulting in increased ventilation [7]. The coupling of increased sympathetic nerve activity (SNA) with increased phrenic nerve activity could be the result of PVN projections to the phrenic motor nucleus in the spinal cord [12]. Activation of beta-2 adrenergic receptors found in human airways causes bronchodilation which aids in increasing ventilation and is caused by the activation of beta-2 adrenergic receptors found in human airways. Beta-2 adrenergic receptors are activated by circulating catecholamines (primarily epinephrine) released by the adrenal medulla upon sympathetic stimulation [11].

Sympathoexcitation augments cardiac output by stimulating the release of norepinephrine from postganglionic sympathetic nerves innervating the SA node, AV node, and the myocardium. Norepinephrine released by these postganglionic sympathetic nerve fibers activates the alpha-1 and beta-1 adrenergic receptors found within the heart. Circulating epinephrine also primarily activates beta-2 adrenergic receptors found in the heart [1]. The release of norepinephrine by postganglionic sympathetic nerves innervating the vascular smooth muscle causes vasoconstriction, thus increasing peripheral resistance. The norepinephrine released by these sympathetic fibers acts on the alpha-1 adrenergic receptors in blood vessels and also the alpha-2 adrenergic receptors [5]. Blood pressure can also be increased by stimulation of the posterior pituitary via projections from the PVN,

which causes the release of vasopressin into the bloodstream by the posterior pituitary. This release of vasopressin increases water retention and causes vasoconstriction [12].

The Paraventricular Nucleus

The PVN is an important site in mediating the autonomic and neuroendocrine regulation of several physiological functions. The PVN is specifically involved in sympathetic cardiovascular regulation [12]. The PVN is a bilateral structure in the hypothalamus that borders the third ventricle. The PVN stretches rostrocaudal alongside the third ventricle and is the dorsal most component of the thalamic-intralaminar nuclear complex in the rat [13]. Previous studies categorized the neurons within the PVN into two main groups: the magnocellular neurons and parvocellular neurons [12,14]. Magnocellular PVN neurons primarily project to the posterior pituitary gland to release vasopressin and oxytocin. Parvocellular PVN neurons are more diverse in function. The medial portion of the PVN parvocellular division projecting to the median eminence has a neuroendocrine function centered around the secretion of thyrotropin-releasing hormone and corticotropin-releasing hormone into the hypophyseal portal system [14]. The medial portion alongside the dorsal, ventral, and posterior portions of the PVN parvocellular division all have a major autonomic role with projections to NTS, RVLM, sympathetic preganglionic neurons in the spinal cord, among other areas of the CNS [12].

The PVN plays a significant role in mediating the sympathetic response to hypoxia. Afferent inputs from chemoreceptors reach the NTS and are relayed to the PVN and other CNS sites. Studies have shown that the PVN contributes significantly to the sympathetic

response to hypoxia primarily by increasing ventilation, heart rate, and blood pressure [12,13,15]. The PVN does not appear to play a significant role in mediating the response to hypercapnia [12,16]. Increased blood volume has also been shown to inhibit PVN activity. Decreased blood volume (hypovolemia) augments general sympathetic activity, however, the PVN only plays a minor role in this response to hypovolemia [17].

The PVN plays an important role in maintaining adequate blood pressure in the event of sustained dehydration. Studies suggest that this increased PVN activity is a result of an increase in osmolarity during dehydration and not the decreased blood volume component of dehydration [17]. The PVN can affect blood pressure via the neuroendocrine route by stimulating the release of vasopressin by the posterior pituitary gland into the bloodstream which causes vasoconstriction and fluid retention [12,14]. It has also been shown that the PVN mediates the control of blood pressure its connections with the RVLM. The PVN has been shown to have some involvement with the baroreflex decreases in SNA by specifically inhibiting lumbar SNA [17].

Afferent Inputs to the PVN

The PVN receives afferent inputs from the brainstem, other hypothalamic nuclei, and various other structures in the CNS. From the medulla, the NTS directly provides the PVN with afferent input integrated from chemoreceptors and baroreceptors. A1 and C1 cell groups from the ventrolateral medulla along with the A2 and C2 cell groups of the dorsal vagal complex also send projections to the PVN. Furthermore, the A5 cell group, A6 cell group (locus coeruleus), and the parabrachial nucleus of the pons all send

projections to the PVN [12, 17-18]. Inputs to the PVN from other hypothalamic subnuclei come from the dorsomedial nucleus, suprachiasmatic nucleus, arcuate nucleus, median preoptic nucleus, and the perifornical area. The inputs from these areas to the PVN are related to emotional stress, circadian rhythms, leptin and insulin levels, osmoregulation, and thermoregulation [18]. Some notable areas outside of the brainstem and hypothalamus that send projections to the PVN include the subfornical organ, organum vasculosum lamina terminalis, and the bed nucleus of the stria terminalis. These areas relay information relating to angiotensin II levels, blood osmolarity, and emotional stress. The PVN also receives direct projections from the dorsal horn of the spinal cord via the spinothalamic tract which primarily carries information from nociceptors regarding painful stimuli [12,17,18].

Efferent Projections from the PVN

The PVN sends efferent projections to key neuroendocrine CNS control sites, various autonomic regulatory sites, and directly to the spinal cord. The PVN's efferent projections to brainstem autonomic regulatory sites include projections to the midbrain, pons, and medulla. The PVN efferent projections to the midbrain include projections to the central gray matter/periaqueductal gray and to the Edinger-Westphal nucleus [12,17,18]. In the pons, the PVN projects to the pedunculopontine tegmental nucleus, locus coeruleus, and parabrachial nucleus. In the medulla, the PVN projects to the NTS, dorsal motor nucleus of the vagus, caudal pressor area, nucleus ambiguus, pre-B complex, and the RVLM. Finally, the spinally projecting neurons of the PVN project to the IML primarily

to the T1-T3 and T9-L3 spinal levels. A portion of these spinally projecting PVN neurons send collaterals to the RVLM. Studies have also suggested that the PVN sends projections to the phrenic motor neurons in the cervical spinal levels [12,17,18].

The Rostral Ventrolateral Medulla

The RVLM is a major site in the brainstem responsible for the sympathetic regulation of cardiac output and blood pressure. The RVLM is a dense column of cells running longitudinally near the ventral surface of the medulla. It is located ventral to the retrofacial nucleus in the medulla. The RVLM is bordered rostrally by the facial motor nucleus, medially by the gigantocellular reticular formation, laterally by the trigeminal nucleus, and caudally by the lateral reticular nucleus [19,20]. C1 adrenergic neurons are found throughout the RVLM and play a significant role in cardiovascular function. These RVLM C1 neurons can be subcategorized into three groups based on where they send projections to. Various non-C1 neurons also make up the RVLM which may also aid in its cardiovascular functions [19].

The RVLM plays an essential role in maintaining blood pressure through its spinal projections to sympathetic preganglionic neurons. Through its spinal projections, the RVLM can in turn affect vasomotor tone, cardiac output, and adrenomedullary catecholamine release [21,22]. Studies have shown that excitation of the presympathetic RVLM neurons increased cardiovascular-related sympathetic nerve activity [21,22]. The increased sympathetic activity to vascular smooth muscle and the heart increases vascular

resistance/vasoconstriction and heart rate. Inhibition of the RVLM by lesions or by microinjections of inhibitory neurotransmitters decreases blood pressure [21].

The RVLM is notably involved in the arterial baroreflex in which sympathetic activity is maintained on a moment-to-moment basis. Increases in blood pressure stimulate arterial baroreceptors and increase the firing frequency to the NTS. The NTS projects to the GABAergic-CVLM neurons which decreases the tonic firing of the RVLM, thus decreasing sympathetic outflow to the heart and blood vessels. A decrease in blood pressure reduces the firing frequency of the baroreceptor afferents and increases the RVLM sympathetic outflow to the heart and blood vessels to restore adequate blood pressure [9, 21-23].

The RVLM is also an important component of the chemoreflex pathway. Chemoreceptor input reaches the RVLM through the same essential pathway that the baroreceptor input takes, only the NTS projections regarding chemoreceptor inputs bypass the CVLM to project directly to the RVLM. The difference is that, unlike increased baroreceptor input, augmented chemoreceptor input (triggered by hypoxia or hypercapnia) results in excitation of the RVLM, which in turn triggers an increase in heart rate and blood pressure. Studies have shown that inhibition or destruction of the RVLM results in a loss of these cardiovascular reflexes, indicating that the RVLM is a vital part of these reflex pathways [22-23].

Afferent Inputs to the RVLM

The RVLM receives various afferent inputs from brainstem regions, higher brain regions, and the spinal cord as demonstrated by several anatomical studies [9,22,24]. In the medulla, afferent inputs to the RVLM arise from the NTS, CVLM, medullary raphe nuclei, Botzinger complex, pre-Botzinger complex, lateral tegmental field, nucleus propositus (also found in the pons), medullary trigeminal nucleus, and the medullary vestibular nucleus [9,22,24]. From the pons, the RVLM receives afferent input from the locus subcoeruleus nucleus, Kolliker-Fuse/subparabrachial nucleus, and the medial and lateral parabrachial nuclei. Afferent inputs to the RVLM also arise from the periaqueductal gray/central gray matter and the A5 cell group located in the midbrain of the brainstem. The higher brain regions that send afferent input to the RVLM primarily include the hypothalamus and the amygdala. From the hypothalamus, the RVLM receives afferent input from the PVN, the DMH, and the lateral hypothalamic area. From the amygdala, the RVLM receives afferent input from the central amygdaloid nucleus [9,22,24]. Spinobulbar neurons also directly innervate the RVLM. The information carried to the RVLM from the spinal cord primarily arises from skeletal muscle receptors and skin nociceptors [9].

Efferent Projections from the RVLM

The RVLM sends efferent projections primarily to areas within the brainstem, hypothalamus, and spinal cord. Within the brainstem, the RVLM projects to a few key areas in the medulla, pons, and midbrain. In the medulla, the RVLM sends projections to the NTS and to the dorsal motor nucleus of the vagus (DMV). The RVLM also sends

efferent projections to the area of the dorsolateral pons. The midbrain periaqueductal gray/central gray matter receives projections from the RVLM. In the hypothalamus, the RVLM projects to the PVN, the supraoptic nuclei, median preoptic nucleus, and to the DMH. Spinal projecting neurons from the RVLM synapse with sympathetic preganglionic neurons in the IML of the thoracolumbar spinal sections [9,19].

CHAPTER THREE

METHODS

Animals

Three adult male Sprague-Dawley rats (Envigo, Indianapolis, IN) weighing 250-300g were used for this study. The procedures and protocols described below are in accord with the National Institutes of Health guidelines and were approved by the Institutional Animal Care and Use Committee at East Tennessee State University. Rats were maintained in our animal facility in standard conditions of light (12-h light/dark cycle) and temperature (22 °C).

Surgical Preparations

Rats were initially anesthetized in an induction chamber using 4-5% isoflurane in O₂ until an adequate anesthetic state was confirmed by the absence of a withdrawal response to painful stimuli in the form of a tail pinch. The fur around the skull and neck was then trimmed and the rats were weighed. Rats were then placed in the supine position with their heads secured into a stereotaxic apparatus (Kopf Instruments, Tujunga, CA) and isoflurane anesthesia was reduced to 2% and resumed through the use of a nose cone. Body temperature was monitored with a rectal thermometer and maintained at 37 °C with a servo-controlled heating lamp. The dorsal surface of the head and neck was then cleaned with betadine and alcohol. A 1.5 cm incision was made in the skin over the occipital bone of the skull. Tissue and membrane were then cleared exposing the occipital bone. An occipital craniotomy was performed in which a small burr hole was made exposing the dorsal surface of the cerebellum at the level of the RVLM.

RVLM Microinjections

Bilateral microinjections of four different FluoSpheres™ into the RVLM was performed using a Nanoject III (Drummond Scientific, Broomall, PA) affixed to the stereotaxic apparatus. A small glass microinjection pipette with a tip diameter of 20-30 µm was used in conjunction with the Nanoject III (Drummond Scientific, Broomall, PA). The glass pipette was advanced into the region of the RVLM while being monitored with a surgical microscope. 100 nanoliters of each FluoSphere™ were injected bilaterally into its assigned rostral-caudal area and the glass pipette was left in place for ~1 minute to ensure adequate diffusion of the retrograde tracer. In the left RVLM, green FluoSpheres™ (505/515), blue FluoSpheres™ (365/415), and red FluoSpheres™ (565/580) were injected (100 nL) in rostral-caudal order. In the right RVLM, only far-red FluoSpheres™ (660/680) were injected (100 nL). After the injections, the overlying membrane and tissue was sutured, and the wound was stapled closed [25].

Recovery

Following the surgical procedures, rats were administered the NSAID analgesic – meloxicam via subcutaneous injection at a dose of 1mg/kg. Rats were then placed back into cages and monitored for ~30 minutes while they regained consciousness to ensure they were healthy and recovered. Rats were then returned to the isolation room in the vivarium and were monitored daily for one week.

Perfusion

It has been shown that 5-7 days is sufficient enough time for the retrograde tracers to travel to the PVN. A week after receiving microinjections, rats were transcardially

perfused using paraformaldehyde under isoflurane anesthesia. Rats were initially anesthetized in an induction chamber with 4-5% isoflurane in O₂ and then transitioned to a nose cone. Adequate depth of anesthesia was again assessed and confirmed by the absence of withdrawal response following a tail pinch. A thoracotomy was then performed exposing the heart. The right atrium was cut to allow for drainage of the perfusion fluids to drain into a biosafety hazard approved receptacle. A metal cannula with 18" of attached silicone tubing was inserted into the ascending aorta through the left ventricle. Cold buffered heparin-saline (300 mL, 60 mL/min) was used as the rinse/wash agent for the perfusion. Cold, fresh, buffered 4% paraformaldehyde (300 mL, 60 mL/min) was then used as the fixative agent for the perfusion. Following the perfusion, brains and brain stems were quickly removed and post-fixed in 4% paraformaldehyde for 24 hours. After the post-fixation, brains and brain stems were cryoprotected by soaking in a 30% sucrose solution for 48 hours [26].

Preparing Brain and Brainstem Sections

Cryoprotected brains and brainstems were sectioned on a freezing microtome. Brain stem sections (40 µm) were cut at the level of the RVLM to verify the microinjection site. For hypothalamic PVN sections, every other 40 µm section was collected from the posterior body of the anterior commissure to the posterior hypothalamus [27]. Brain and brainstem sections were placed into a 24 well tray containing phosphate buffered saline (PBS). Brain and brainstem sections were then mounted onto glass slides and cover slipped.

Analysis

Slides were dried overnight and then examined with a fluorescence Olympus BH2 microscope (Center Valley, PA) for retrograde tracing/labeling in the PVN. A rat brain

atlas was used to determine which sections contained the PVN. The PVN was defined in stereotaxic coordinates as the bilateral structure bordering the third ventricle from bregma -0.60mm to bregma -2.28mm [27]. We counted neurons labeled with fluorescence within the area of the PVN for each 40 μ m section. A digital camera affixed to the fluorescent microscope was used to project images to a large monitor to facilitate the counting of neurons while ensuring none were double counted. Images of selected brain sections were obtained using an Olympus BX63 automated fluorescence microscope (Center Valley, PA) equipped with a Hamamatsu C11440 digital camera (Bridgewater, NJ).

CHAPTER FOUR

RESULTS

Identification of PVN Subnuclei Containing RVLM-Projecting Neurons

To identify neurons within the PVN that send axonal projections to the RVLM, we injected four different FluoSpheres™ into the RVLM. Green (505/515), blue (365/415), and red (565/580) FluoSpheres™ were injected rostro-caudally into the left RVLM and far-red (660/680) FluoSpheres™ were injected into the right RVLM. Histological analysis showed that only the red and green fluosphere microinjections were located within the left RVLM (figure 1).

Figure 1

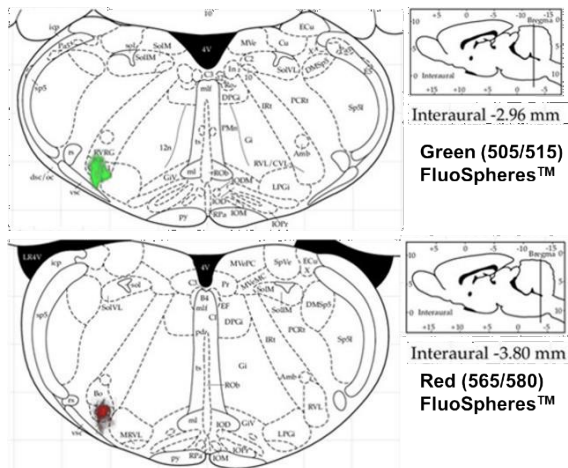
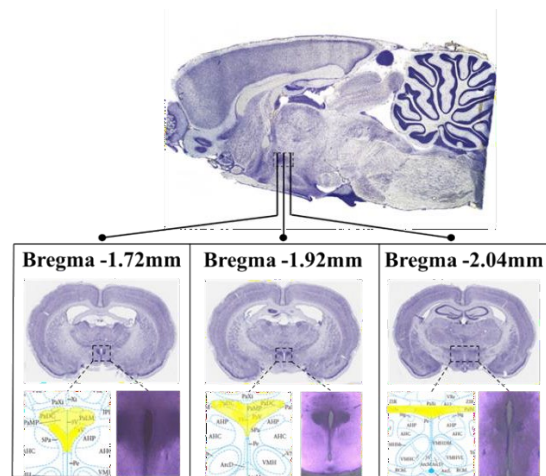


Figure 2



Following the microinjections, we inspected the fluorescent retrograde labeling within the PVN. Of the seven subnuclei within the PVN, we identified four that contained retrogradely labeled neurons, these being the ventral parvocellular, dorsal cap parvocellular, medial parvocellular, and the posterior parvocellular subnuclei. These four

subnuclei expressed the best labeling at three levels which are shown by the representative Nissl stain images (figure 2). Neurons in these PVN subnuclei exhibited fluorescent retrograde labeling with only the green (505/515) and red (565/580) tracers. There was no retrograde labeling visible at any level within the PVN with either the blue (365/415) or far-red (660/680) tracers. There was also no labeling of any kind in the remaining three PVN subnuclei which includes the anterior parvocellular, medial magnocellular, and lateral magnocellular subnuclei.

The mean number of RVLM-projecting PVN neurons identified was $369 (\pm 37.4)$. Of these, $293.3 (\pm 57.8)$ were labeled with the red (565/580) fluosphere and $75.7 (\pm 39.5)$ were labeled with the green (505/515) fluosphere. Regarding laterality, 88.4% of labeled neurons were located in the ipsilateral PVN, while 11.6% of the labeled neurons were located in the contralateral PVN. The ventral parvocellular (PaV) subnucleus contained a mean of $15 (\pm 2.5)$ RVLM-projecting neurons. Of these, $13.7 (\pm 3.4)$ neurons were labeled red and $1.3 (\pm 0.9)$ were labeled green (figure 3). The dorsal cap parvocellular (PaDC) subnucleus contained a mean of $44.3 (\pm 15.1)$ RVLM-projecting neurons. Of these, $36 (\pm 14.1)$ neurons were labeled red and $8.3 (\pm 5.2)$ were labeled green (figure 4).

Figure 3: Ventral Parvocellular Subnucleus

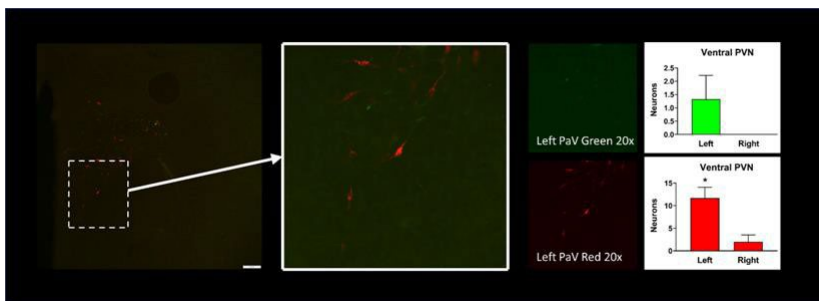
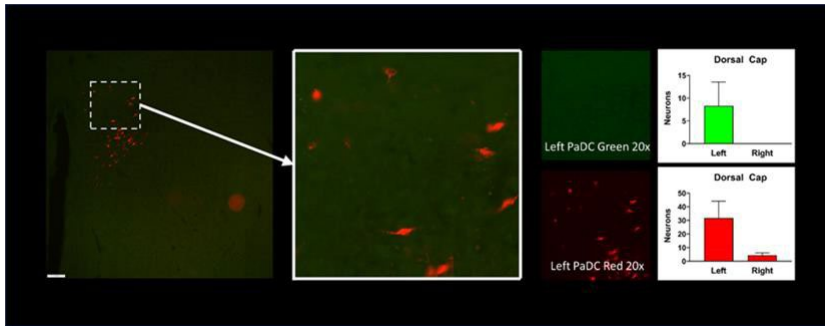


Figure 4: Dorsal Cap Parvocellular Subnucleus



The medial parvocellular (PaMP) subnucleus contained a mean of 223.7 (± 28.9) RVLM-projecting neurons. Of these, 169.3 (± 21.1) neurons were labeled red and 54.3 (± 31.2) were labeled green (figure 5). The posterior parvocellular (PaPO) subnucleus contained a mean of 86 (± 22.1) RVLM-projecting neurons. Of these, 74.3 (± 26) neurons were labeled red and 11.7 (± 6) were labeled green (figure 6). In all four of the subnuclei, the majority of the RVLM-projecting neurons were labeled with the red (565/580) FluoSpheresTM and were found on the ipsilateral side (figure 7).

Figure 5: Medial Parvocellular Subnucleus

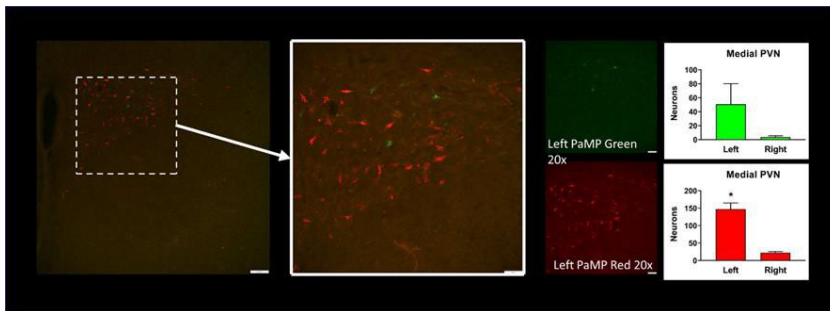


Figure 6: Posterior Parvocellular Subnucleus

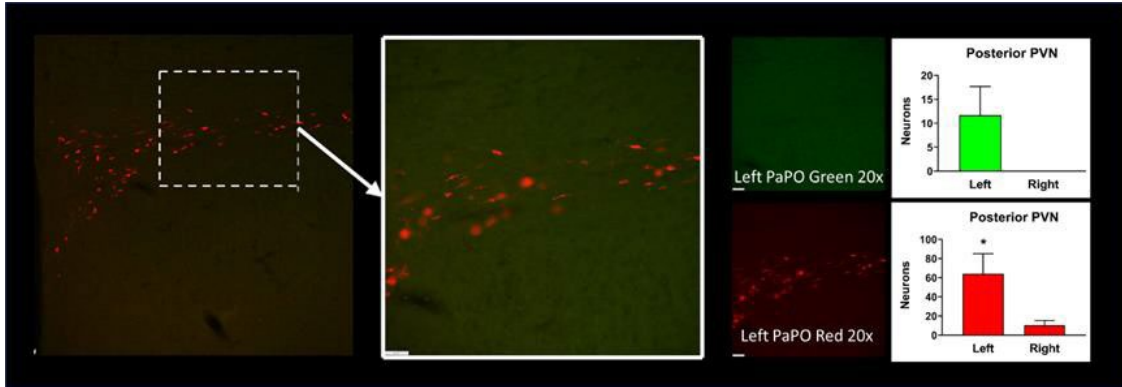
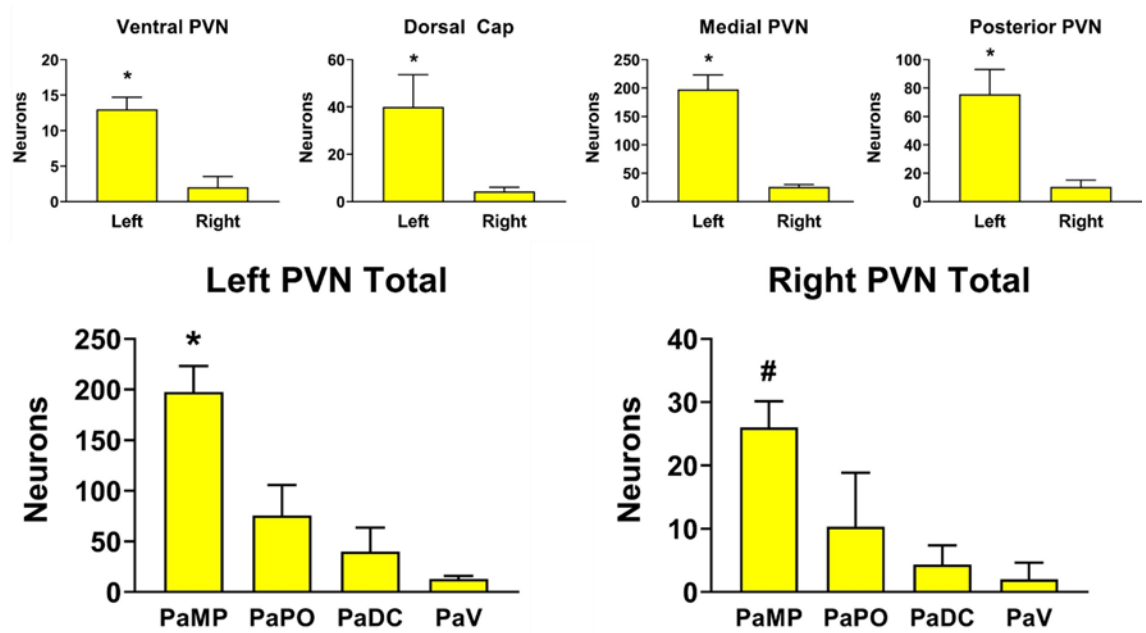


Figure 7: Summary Retrograde Labeling



CHAPTER FIVE

DISCUSSION

In past anatomical studies, it has been demonstrated that the PVN sends axonal projections to the RVLM. These RVLM-projecting neurons have been shown to originate primarily from within the parvocellular division of the PVN. Furthermore, these PVN-RVLM projections have also been shown to be predominately ipsilateral [12,28]. The results from the present study support these findings in that all of the labeled neurons found were parvocellular and were ipsilateral to the brainstem injection site. Our study further characterized the distribution of these RVLM-projecting neurons within the seven subnuclei of the PVN. Using fluorescent retrograde tracing, we identified four specific subnuclei that contained RVLM-projecting neurons which include the ventral, dorsal cap, posterior, and medial parvocellular subnuclei. The medial parvocellular subnucleus contained the majority of these RVLM-projecting neurons.

The sympathetic role of these PVN neurons in cardiovascular regulation has been investigated by several studies. These studies have shown that these RVLM-projecting PVN neurons terminate at the neurons within the RVLM that project to the IML of the spinal cord [17,22,29-32]. These sympathetic RVLM premotor neurons synapse in the IML with preganglionic neurons involved with cardiovascular regulation. This suggests that the PVN has an important role in mediating the sympathetic responses produced by the RVLM.

The PVN is an autonomic premotor nucleus that has direct projections to the IML as well as collaterals that branch to the IML-projecting RVLM neurons. As such, the PVN can directly regulate cardiovascular activity independent of the RVLM [28].

The results from our study also suggest that the different fluorescent retrograde tracers used (FluoSpheres™) did not act in an equally efficient manner. All of these FluoSpheres™ used had carboxylate-modified coupling surfaces but had different colors of dye used for labeling. The red (565/580) FluoSphere™ was the most robust at labeling neurons. It accounted for a majority of the labeling and was very easy to visualize under a fluorescent microscope. The green (505/515) FluoSphere™ was less effective than the red but more effective than the blue and far-red tracers. The green tracer still exhibited neuronal labeling but was harder to visualize than the red tracer. The green could have been harder to see in general, or it could be that it was not taken up as a tracer as well as the red was. Initially, we thought that this may be caused by the injection site of the green tracer being more rostral to the red which would suggest that the majority of RVLM-projecting PVN neurons innervate the medial aspect of the RVLM. However, this is speculative since the injection sites of the green and red overlapped in several instances. A smaller volume of injectant could be useful in the future for keeping each tracer isolated to its own area within the RVLM in order to better differentiate between the effectiveness of each.

The blue (365/415) and the far-red (660/680) FluoSpheres™ did not exhibit any labeling at any level of the PVN. In the case of the blue tracer, this is likely to be the result of a problem with the tracer itself. The blue tracer was confirmed to be injected into the area of the RVLM in our experiments, however, it produced no labeling in the PVN. The

only differing factor of this tracer is that it was of smaller size (.02 μ m instead of .04 μ m) than the other tracers. A similar type of tracer that was of the same size labeled with rhodamine had been previously shown to be effective as a neuronal retrograde tracer [33]. This could mean that the problem is with the type of blue dye used that makes it difficult to visualize. The lack of ability to produce labeling in the PVN with the far-red tracer was most likely due to the location of the injection site and not a problem with the tracer itself. Examination of the brainstem injection sites suggests that the far-red tracer injection in the right brainstem was too medial to enter the area of the RVLM.

Conclusion

Inputs to the PVN and RVLM mediate changes in sympathetic tone that affect heart rate and blood pressure. Activation of neurons within the PVN that project to the RVLM can lead to an increase in sympathetic activity resulting in elevated blood pressure. The specific subnuclei that contain these RVLM-projecting neurons were identified in this study. The anatomic data provided by this study will serve as important preliminary data for future studies investigating the functional and histochemical properties of these neurons.

APPENDIX A

FIGURE 1

Brain Stem Microinjections Sites

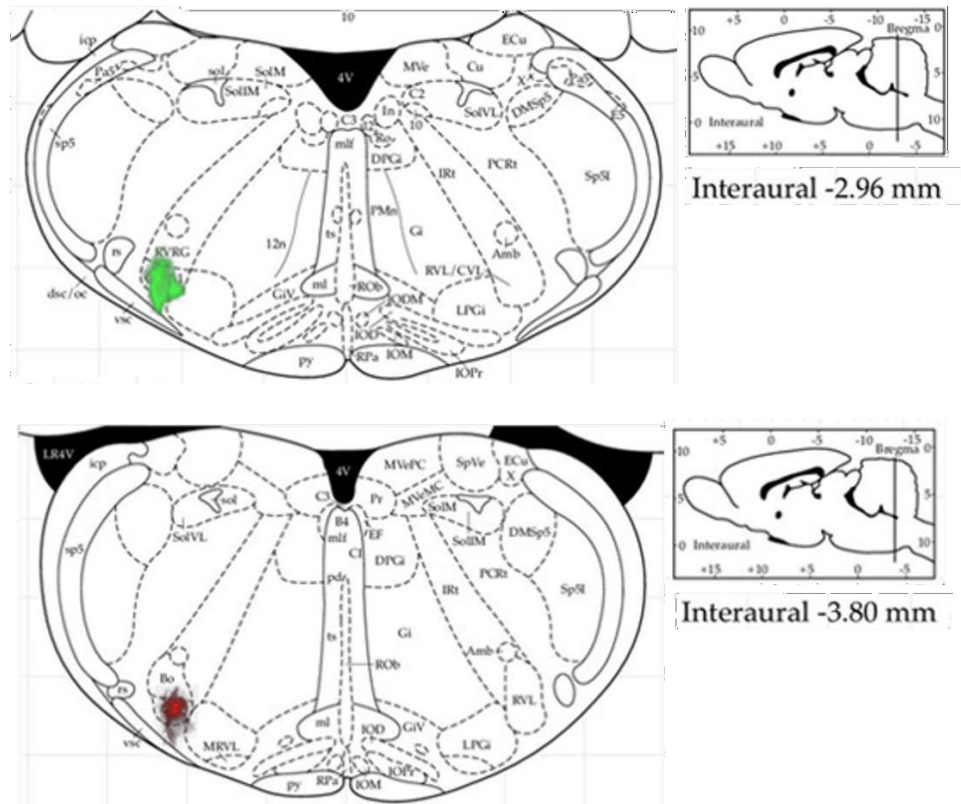


Figure 1: Composite image showing the brain stem injection sites of both the green (top) and red (bottom) tracers at their respective levels within the brainstem. The green (505/515) tracer was injected more rostrally into the RVL. The red (565/580) tracer was injected more caudally into the RVL.

FIGURE 2

Representative Nissl Stain Images of PVN

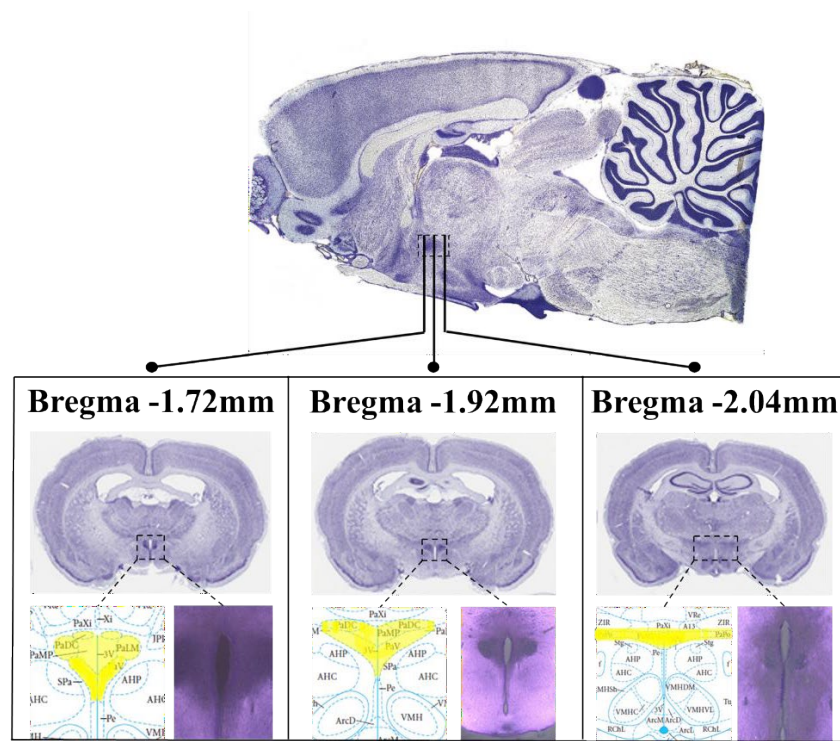


Figure 2: Representative image for one rat showing the area of the PVN in the sagittal section with representative Nissl stain images corresponding to the levels of the PVN that we took actual images of the neuronal labeling. Also shown is the corresponding image from the brain atlas with the PVN subnuclei highlighted in yellow.

FIGURE 3

Ventral Parvocellular Subnucleus (PaV) at Bregma -1.72mm

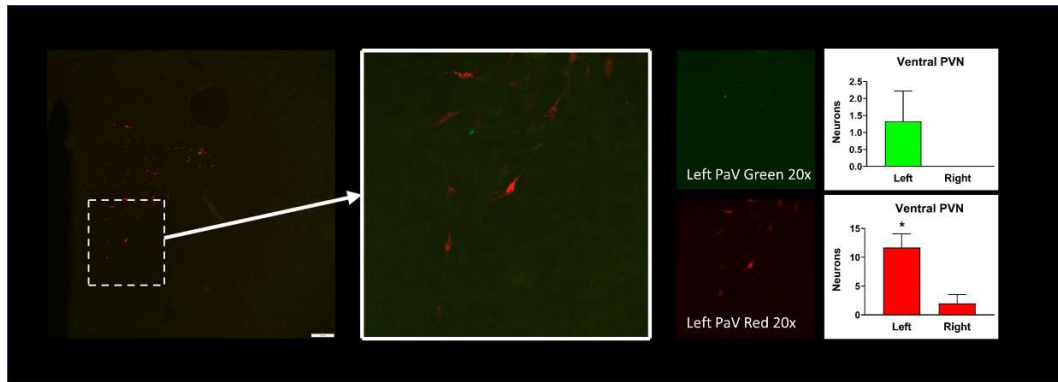
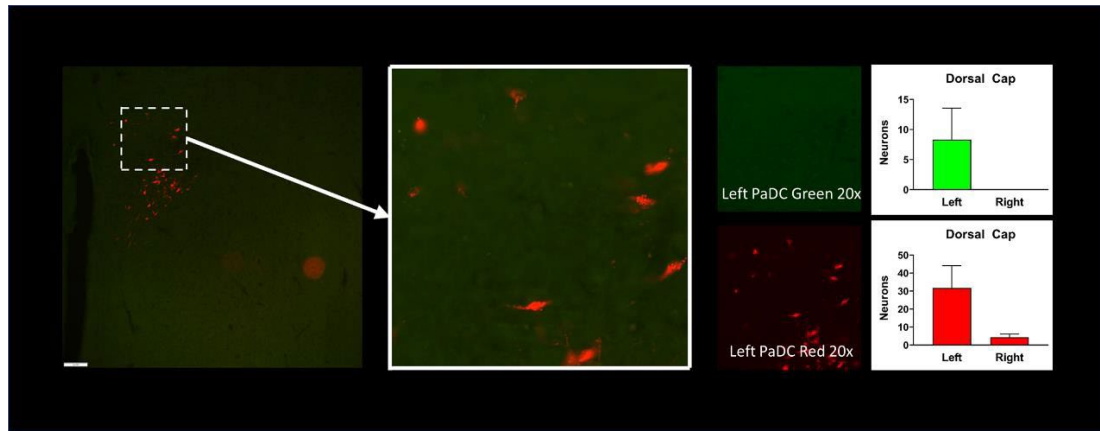


Figure 3: Representative image for one rat showing the PVN emphasizing the ventral parvocellular subnucleus (PaV) – (left 10x, right 20x merged) showing differential fluorescence. PaV is outlined in white. Grouped data showing the mean number of green (A) and red (B) neurons in the ipsilateral and contralateral ventral subnucleus of the PVN.

FIGURE 4

Dorsal Cap Parvocellular Subnucleus (PaDC) at Bregma -1.92mm



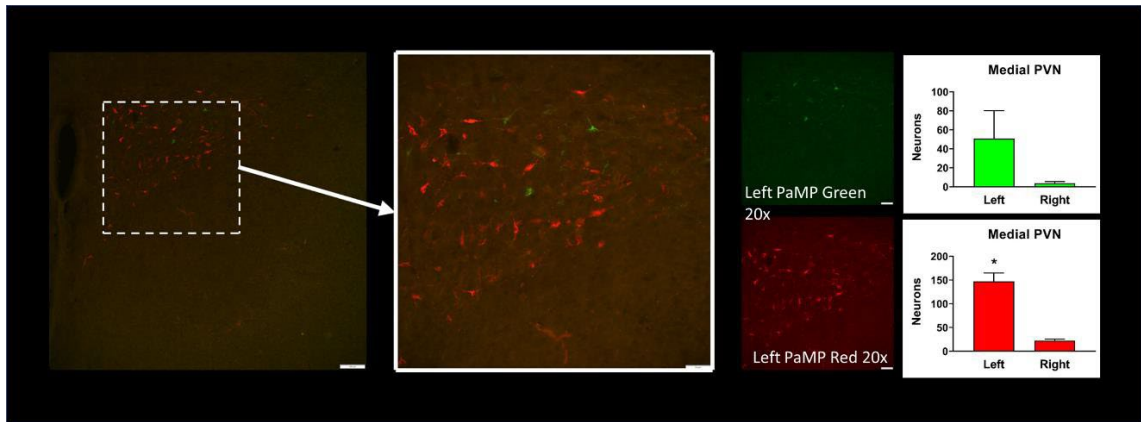
A.

B.

Figure 4: Representative image for one rat showing the PVN emphasizing the dorsal cap parvocellular subnucleus (PaDC) – (left 10x, right 20x merged) showing differential fluorescence. PaDC is outlined in white. Grouped data showing the mean number of green (A) and red (B) neurons in the ipsilateral and contralateral dorsal cap subnucleus of the PVN.

FIGURE 5

Medial Parvocellular Subnucleus (PaMP) at Bregma -1.92mm



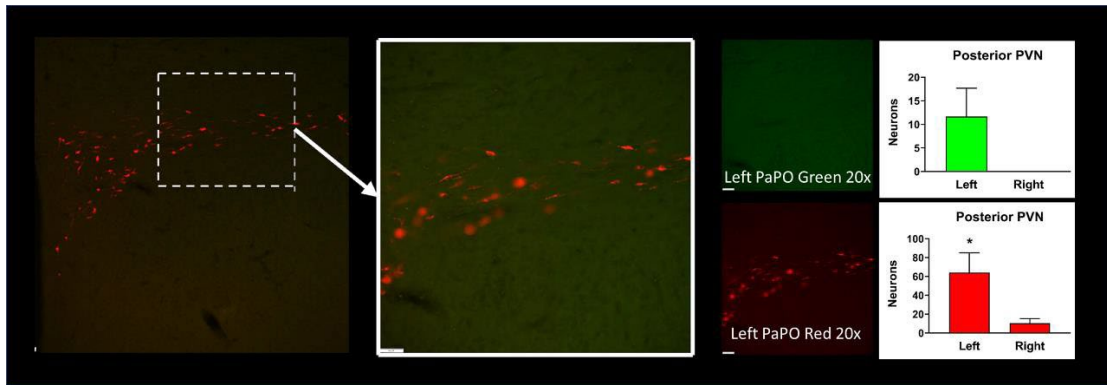
A.

B.

Figure 5: Representative image for one rat showing the PVN emphasizing the medial parvocellular subnucleus (PaMP) – (left 10x, right 20x merged) showing differential fluorescence. PaMP is outlined in white. Grouped data showing the mean number of green (A) and red (B) neurons in the ipsilateral and contralateral medial subnucleus of the PVN.

FIGURE 6

Posterior Parvocellular Subnucleus (PaPO) at Bregma -2.04mm



A.

B.

Figure 6: Representative image for one rat showing the PVN emphasizing the posterior parvocellular subnucleus (PaPO) – (left 10x, right 20x merged) showing differential fluorescence. PaPO is outlined in white. Grouped data showing the mean number of green (A) and red (B) neurons in the ipsilateral and contralateral posterior subnucleus of the PVN.

FIGURE 7

Summary Retrograde Labeling

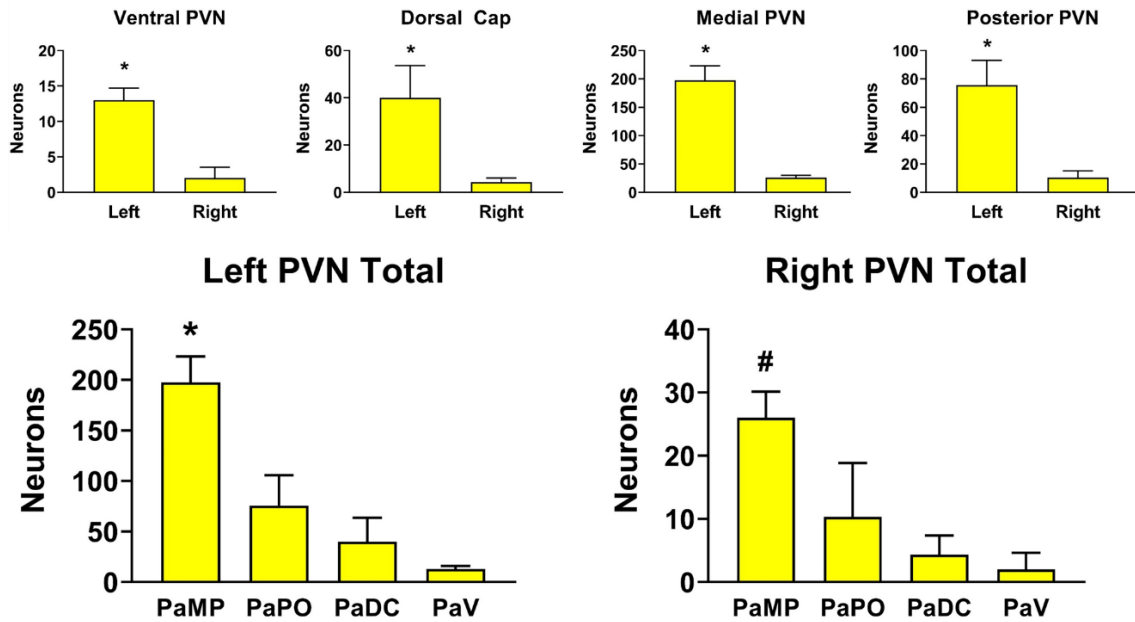


Figure 7: Summary data of the combined red and green retrograde tracing in the PVN showing the distribution of RVLM-projecting neurons within the different subnuclei of the PVN, shown in yellow. PaMP (Medial PVN), PaPO (Posterior PVN), PaDC (Dorsal Cap), PaV (Ventral PVN).

REFERENCES

1. Gordan R, Gwathmey JK, Xie LH. Autonomic and endocrine control of cardiovascular function. *World J Cardiol.* 2015;7(4):204-214.
2. Malpas SC. Sympathetic nervous system overactivity and its role in the development of cardiovascular disease. *Physiol Rev.* 2010;90(2):513-557.
3. Vincent JL. Understanding cardiac output. *Crit Care.* 2008;12(4):174.
4. Borovac JA, D'Amario D, Bozic J, Glavas D. Sympathetic nervous system activation and heart failure: Current state of evidence and the pathophysiology in the light of novel biomarkers. *World J Cardiol.* 2020;12(8):373-408.
5. Thomas GD. Neural control of the circulation. *Advances in Physiology Education.* 2011;35:1,28-32
6. Lewis MJ, Short AL, Lewis KE. Autonomic nervous system control of the cardiovascular and respiratory systems in asthma. *Respiratory Medicine.* 2006;100(10):1688-1705.
7. Schultz HD, Li YL, Ding Y. Arterial Chemoreceptors and Sympathetic Nerve Activity: Implications for Hypertension and Heart Failure. *Hypertension.* 2007;50(1):6-13.

8. Charkoudian N, Rabbitts JA. Sympathetic neural mechanisms in human cardiovascular health and disease. *Mayo Clin Proc.* 2009;84(9):822-830.
9. Dampney RAL. Central neural control of the cardiovascular system: current perspectives. *Advances in Physiology Education.* 2016;40(3):283-296.
10. Andrade DC, Haine L, Toledo C, et al. Ventilatory and Autonomic Regulation in Sleep Apnea Syndrome: A Potential Protective Role for Erythropoietin? . *Frontiers in Physiology* . 2018;9. doi:10.3389/fphys.2018.01440
11. McCorry LK. Physiology of the autonomic nervous system. *Am J Pharm Educ.* 2007;71(4):78.
12. Kc P, Dick TE. Modulation of Cardiorespiratory Function Mediated by the Paraventricular Nucleus. *Respiratory physiology & neurobiology* 174.1 (2010): 55–64.
13. Feetham CH, O'Brien F, Barrett-Jolley R. Ion Channels in the Paraventricular Hypothalamic Nucleus (PVN); Emerging Diversity and Functional Roles. *Frontiers in Physiology.* 2018. doi:doi.org/10.3389/fphys.2018.00760
14. Qin C, Li J, Tang K. The Paraventricular Nucleus of the Hypothalamus: Development, Function, and Human Diseases. *Endocrinology* . 2018;159(9):3458-3472.
15. Ruyle BC, Martinez D, Heesch CM, Kline DD, Hasser EM. The PVN enhances cardiorespiratory responses to acute hypoxia via input to the nTS. *Am J Physiol*

Regul Integr Comp Physiol. 2019;317(6):R818-R833.

doi:10.1152/ajpregu.00135.2019

16. Guyenet PG. Regulation of breathing and autonomic outflows by chemoreceptors. *Compr Physiol.* 2014;4(4):1511-1562.
17. Dampney RA, Michelini LC, Li DP, Pan HL. Regulation of sympathetic vasomotor activity by the hypothalamic paraventricular nucleus in normotensive and hypertensive states. *Am J Physiol Heart Circ Physiol.* 2018;315(5):H1200-H1214.
18. Benarroch EE. Paraventricular nucleus, stress response, and cardiovascular disease. *Clinical autonomic research : official journal of the Clinical Autonomic Research Society.* 2005;15(4):254-263.
19. Guyenet PG, Stornetta RL, Holloway BB, Souza GM, Abbott SB. Rostral Ventrolateral Medulla and Hypertension. *Hypertension.* 2018;72(3):559-566.
20. Sugiyama Y, Suzuki T, Yates BJ. Role of the rostral ventrolateral medulla (RVLM) in the patterning of vestibular system influences on sympathetic nervous system outflow to the upper and lower body. *Exp Brain Res.* 2011;210(3-4):515-527.
21. Kumagai H, Oshima N, Matsuura T, et al. Importance of rostral ventrolateral medulla neurons in determining efferent sympathetic nerve activity and blood pressure. *Hypertens Res.* 2012;35(2):132-141.

22. Dampney RA. Functional organization of central pathways regulating the cardiovascular system. *Physiol Rev.* 1994;74(2):323-364.
23. Dampney RA, Coleman MJ, Fontes MA, et al. Central mechanisms underlying short- and long-term regulation of the cardiovascular system. *Clin Exp Pharmacol Physiol.* 2002;29(4):261-268.
24. Dempsey B, Le S, Turner A, et al. Mapping and Analysis of the Connectome of Sympathetic Premotor Neurons in the Rostral Ventrolateral Medulla of the Rat Using a Volumetric Brain Atlas. *Front Neural Circuits.* 2017;11:9. Published 2017 Mar 1.
25. Li DP, Pan HL. Plasticity of GABAergic control of hypothalamic presympathetic neurons in hypertension. *Am J Physiol Heart Circ Physiol.* 2006;290(3):H1110-H1119.
26. Zahner MR, Schramm LP. Spinal regions involved in baroreflex control of renal sympathetic nerve activity in the rat. *Am J Physiol Regul Integr Comp Physiol.* 2011;300(4):R910-R916.
27. Paxinos G, Watson C. *The Rat Brain in Stereotaxic Coordinates: Hard Cover Edition.* 6th ed. San Diego, CA: Academic Press; 2006.
28. Badoer E. Proceedings of the Australian Physiological and Pharmacological Society Symposium: The Hypothalamus HYPOTHALAMIC PARAVENTRICULAR NUCLEUS AND CARDIOVASCULAR

REGULATION. *Clinical and Experimental Pharmacology and Physiology*.
2001;28(1-2):95-99. doi:10.1046/j.1440-1681.2001.03413.x.

29. Coote JH, Yang Z, Pyner S, Deering J. Control of sympathetic outflows by the hypothalamic paraventricular nucleus. *Clin Exp Pharmacol Physiol*. 1998;25(6):461-463. doi:10.1111/j.1440-1681.1998.tb02235.x
30. Zahner MR, Pan HL. Role of paraventricular nucleus in the cardiogenic sympathetic reflex in rats. *Am J Physiol Regul Integr Comp Physiol*. 2005;288(2):R420-R426. doi:10.1152/ajpregu.00563.2004
31. Pyner S, Coote JH. Identification of an efferent projection from the paraventricular nucleus of the hypothalamus terminating close to spinally projecting rostral ventrolateral medullary neurons. *Neuroscience*. 1999;88(3):949-957. doi:10.1016/s0306-4522(98)00255-3
32. Tjen-A-Looi SC, Guo ZL, Fu LW, Longhurst JC. Paraventricular Nucleus Modulates Excitatory Cardiovascular Reflexes during Electroacupuncture. *Sci Rep*. 2016;6:25910. Published 2016 May 16. doi:10.1038/srep25910
33. Katz LC, Burkhalter A, Dreyer WJ. Fluorescent latex microspheres as a retrograde neuronal marker for in vivo and in vitro studies of visual cortex. *Nature*. 1984;310(5977):498-500. doi:10.1038/310498a0

Fuller Thesis Final

Final Audit Report

2022-04-29

Created:	2022-04-29
By:	Nicolas Fuller (fullernf@etsu.edu)
Status:	Signed
Transaction ID:	CBJCHBCAABAATjLug-HmD7nSVePaklvWIP-gZqcanmtT

"Fuller Thesis Final" History

-  Document created by Nicolas Fuller (fullernf@etsu.edu)
2022-04-29 - 4:57:34 AM GMT
-  Document emailed to Nicolas Fuller (fullernf@etsu.edu) for signature
2022-04-29 - 5:03:53 AM GMT
-  Document emailed to Matthew Zahner (zahner@mail.etsu.edu) for signature
2022-04-29 - 5:03:53 AM GMT
-  Document emailed to Eric Beaumont (beaumont@mail.etsu.edu) for signature
2022-04-29 - 5:03:53 AM GMT
-  Document emailed to Michelle Chandley (chandlem@mail.etsu.edu) for signature
2022-04-29 - 5:03:53 AM GMT
-  Document e-signed by Nicolas Fuller (fullernf@etsu.edu)
Signature Date: 2022-04-29 - 5:05:20 AM GMT - Time Source: server
-  Email viewed by Matthew Zahner (zahner@mail.etsu.edu)
2022-04-29 - 5:06:43 AM GMT
-  Email viewed by Eric Beaumont (beaumont@mail.etsu.edu)
2022-04-29 - 1:33:15 PM GMT
-  Document e-signed by Eric Beaumont (beaumont@mail.etsu.edu)
Signature Date: 2022-04-29 - 1:33:30 PM GMT - Time Source: server
-  Email viewed by Michelle Chandley (chandlem@mail.etsu.edu)
2022-04-29 - 3:13:29 PM GMT
-  Document e-signed by Michelle Chandley (chandlem@mail.etsu.edu)
Signature Date: 2022-04-29 - 3:15:33 PM GMT - Time Source: server

 Document e-signed by Matthew Zahner (zahner@mail.etsu.edu)

Signature Date: 2022-04-29 - 4:33:56 PM GMT - Time Source: server

 Agreement completed.

2022-04-29 - 4:33:56 PM GMT